IOPscience iopscience.iop.org

Home Search Collections Journals About Contact us My IOPscience

Raman studies on spintronics materials based on wide bandgap semiconductors

This article has been downloaded from IOPscience. Please scroll down to see the full text article.

2004 J. Phys.: Condens. Matter 16 S5653

(http://iopscience.iop.org/0953-8984/16/48/023)

View the table of contents for this issue, or go to the journal homepage for more

Download details:
IP Address: 129.252.86.83
The article was downloaded on 27/05/2010 at 19:18

Please note that terms and conditions apply.

INSTITUTE OF PHYSICS PUBLISHING JOURNAL OF PHYSICS: CONDENSED MATTER

J. Phys.: Condens. Matter **16** (2004) S5653–S5660 PII: S0953-8984(04)80276-5

Raman studies on spintronics materials based on wide bandgap semiconductors

H Harima

Department of Electronics and Information Science, Kyoto Institute of Technology, Kyoto 606-8585, Japan

Received 6 May 2004
Published 19 November 2004
Online at stacks.iop.org/JPhysCM/16/S5653
doi:10.1088/0953-8984/16/48/023

Abstract

Structural properties of GaN and ZnO layers doped with magnetic impurities were investigated by Raman scattering. Long-range lattice ordering and local atomic arrangement around magnetic impurities were analysed, and their solubility limit was considered.

For this study, GaN layers doped with Mn and Cr, and ZnO layers doped with Co and V were prepared by molecular beam epitaxy and pulsed laser deposition, respectively. ZnO layers codoped with Ga and N were also studied for the purpose of p-type activation. These samples were observed using a Raman microprobe using visible and deep UV lasers for excitation. The main results are as follows:

In $Ga_{1-x}Mn_xN$ layers, a uniform solid solution was formed for Mn concentration up to $x = 1$–2%. An impurity mode was observed at 585 cm^{-1} and assigned to a local vibrational mode of Mn substituting the Ga site. At higher Mn concentrations, rapid deterioration in lattice ordering occurred. $Ga_{1-x}Cr_xN$ layers showed good lattice ordering up to $x = 3$–5%. The samples showed resonance enhancement of LO-phonon signals when excited by a UV laser at 266 nm (4.7 eV). This indicates the photo-injection of free carriers to a diluted magnetic semiconductor.

ZnO layers codoped with Ga and N showed many impurity modes due to host lattice defects. A strong signal at 580 cm^{-1} showed a characteristic broadening at high concentrations of N and Ga. This suggested the formation of complex centres with N or related defects. $Zn_{1-x}Co_xO$ and $Zn_{1-x}V_xO$ layers formed uniform solid solutions up to $x \sim 5\%$, but precipitation of the secondary phase was observed at $x > \sim 10\%$. These samples presented common defect modes as observed in codoped samples. Our result suggests that the impurity modes in ZnO-based materials can be used as a sensitive probe of host lattice defects induced by the impurity incorporation process.

0953-8984/04/485653+08$30.00 © 2004 IOP Publishing Ltd Printed in the UK

1. Introduction

Wide bandgap semiconductors doped with magnetic impurities are highly promising candidates for diluted magnetic semiconductors (DMS) to realize ferromagnetism at above room temperature [1, 2]. To date, however, both positive and negative experimental results have appeared, suggesting that the sample performance is delicately dependent on the impurity species, their concentration and the growth process [3]. Because of the relatively low miscibility of magnetic elements to semiconductors, it is generally a hard task to prepare uniform solid solutions, and secondary phases have always been suspected as the origin of observed magnetic orderings. Under this situation, it is clear that precise characterization of the structural properties for each sample is indispensable to evaluate the potential of DMS candidates.

Although spectroscopic techniques like IR absorption and Raman scattering have played a large role in characterizing the local atomic arrangement around non-magnetic impurities in a variety of semiconductors [4], similar attempts on DMS candidates are very limited [3]. From this viewpoint, we have conducted Raman scattering experiments on GaN- and ZnO-based materials doped with some magnetic elements. We will focus here on long-range lattice ordering and the local atomic arrangement around the magnetic impurities. In addition, ZnO layers codoped with Ga and N are also examined. This is because p-type activation may be a key step to realizing room temperature ferromagnetism in ZnO-based materials [1, 2], and the codoping technique has been proposed to realize p-type conductivity [5].

2. Experiment

The GaN-based samples were grown by molecular beam epitaxy (MBE) on a sapphire (0001) substrate after deposition of a GaN buffer layer using NH_3 or plasma-enhanced N_2 for the nitrogen source, and elemental sources of metallic elements [6, 7]. The GaMnN and GaCrN layers were grown at 750–850 and 620 °C with thickness 200 and 500 nm, respectively.

The ZnO-based samples were grown by pulsed laser deposition (PLD) in an oxygen atmosphere on sapphire $(11\bar{2}0)$ for V- and Co-doping, and on a glass substrate (Corning 7059) for Ga + N codoping [8, 9]. The growth temperature was 300–600 °C and the thickness was 100–300 nm. In the codoped samples, nitrogen was supplied through a RF radical source using N_2O gas.

Raman scattering was conducted at room temperature using a confocal microscope with an Ar ion laser at 488.0 or 514.5 nm, and the fourth harmonics of a YAG laser at 266 nm for a resonant Raman experiment. Back-scattering configuration from the c-plane was employed, and the scattered light was analysed using a double monochromator with focal length 85 cm equipped with a liquid-N_2-cooled CCD (charge coupled device) detector.

This work is based on collaboration with various structural characterizations for the samples: the concentration of impurity was evaluated by electron probe micro-analysis (EPMA) or secondary ion mass spectrometry (SIMS). X-ray diffraction (XRD) was also conducted to confirm single-phase formation. In some materials, the local atomic arrangement around the impurity was investigated by extended x-ray absorption fine structure (EXAFS).

3. Results and discussion

3.1. GaN doped with Mn and Cr

Figure 1(a) shows Raman spectra of $Ga_{1-x}Mn_xN$ with $x = 0.44\%$ (#A), 1.4% (#B) and 12% (#C) observed using 514.5 nm-laser excitation. For comparison, figure 1(a) contains

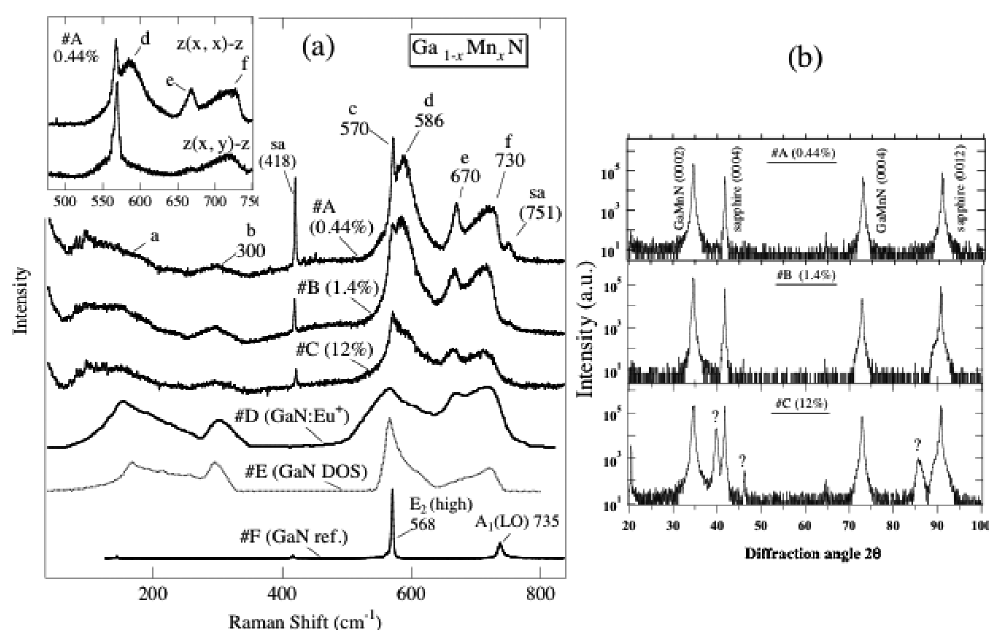

Figure 1. Raman spectra of $Ga_{1-x}Mn_xN$ (a) and their XRD patterns (b). The inset in (a) shows a polarization experiment on #A. The sample #C shows secondary phase signals as denoted by question marks. For reference, (a) contains spectra of high quality GaN (#F), ion-implanted GaN (#D) and a phonon-DOS calculation [10].

typical spectra of high quality GaN (#F) and ion-implanted GaN (#D), both grown by metalorganic chemical vapour deposition (MOCVD), and calculated phonon DOS (density of states) (#E) [10]. The inset shows a polarized spectra of #A, where $z(x, x)$–z and $z(x, y)$–z mean parallel and crossed polarization geometry, respectively. Figure 1(b) shows XRD patterns for the tested samples. There is no phase separation for #A and #B, but #C includes signals due to some secondary phase.

In figure 1(a), the samples #A to C commonly show broad signals due to GaMnN layers at about 100–200, 300, 580–600, 670 and 730 cm^{-1}, which are marked as (a), (b), (d), (e) and (f), respectively. Furthermore, #A shows a sharp peak at 570 cm^{-1} (c) due to the E_2(high) phonon mode of GaN (or GaMnN). Sharp sapphire substrate signals (sa) are also observed, which grow in intensity as the samples become more transparent with decreasing x. The broad features (a), (b) and (f) are well reproduced in an ion-implanted sample of GaN (#D) and resemble its phonon DOS profile (#E) [10]. This means that (a), (b) and (f) are disorder-activated modes that are observed when long-range lattice ordering of the host lattice is lost. In this case, Raman signals show no clear polarization dependence as evidenced for (f) in the inset. By contrast, (d) and (e) show clear polarization dependence. Furthermore, unlike the disorder-activated modes, (d) and (e) become sharp as the Mn content decreases, or the long-range lattice ordering of the host lattice is higher. Taking this polarization dependence into account, we assign (e) to a local vibrational mode (LVM) of GaN related to a vacancy. These interpretations are in line with a detailed investigation by Limmer *et al* on GaN ion-implanted with different elements [11].

Raman spectra of $Ga_{1-x}Mn_xN$ were first reported by Gebicki and his co-workers using free-standing samples grown by re-sublimation [12] and by an ammonothermal method [13]. Their results present similar spectra to those of ion-implanted GaN [10, 11] and of our present phase-separated GaMnN sample (#C). According to the interpretation by Gebicki *et al* [13],

the peaks (a), (b) and (e) in figure 1 are classified as disorder-activated modes, and (f) as the A_1(LO) phonon mode. We agree on their interpretation for (a) and (b), but not for the other signals because of the polarization properties. The peak (d) is a new signal which has not been reported in GaMnN [12, 13] or ion-implanted GaN samples [10, 11]. Here we tentatively assign the peak (d) to LVM of Mn occupying the Ga site because of the following reasons: first, the peak frequency ($\sim$586 cm^{-1}) is close to a rough estimation based on the GaN E_2(high)-phonon frequency with consideration of the reduced-mass difference between the Ga–N and Mn–N pairs, i.e. $\omega_{Mn-N} \sim \omega_{Ga-N}[\mu_{Ga-N}/\mu_{Mn-N}]^{1/2} = 582$ cm^{-1}. Second, as seen in the inset of figure 1, this peak disappears in crossed polarization geometry, which is consistent with the local symmetry around the Mn atom if it occupies the Ga site (C_{3v}, in wurtzite host lattice). Third, this peak was clearly observed in our experiment only in the non-phase-separated samples, #A ($x = 0.44\%$) and #B ($x = 1.4\%$). We consider that the peak (d) is a measure of a uniform solid solution of $Ga_{1-x}Mn_xN$, in which long-range lattice ordering is achieved as a ternary alloy system.

A separate experiment on magnetization properties revealed that our non-phase-separated samples were mainly paramagnetic, while the phase-separated ones were mainly ferromagnetic at low temperature due to Mn-based precipitates [6]. This result agrees with that of Zajac *et al* [13]; their sample was dominated by paramagnetic behaviour, while the secondary phase components (Mn_xN_y) made ferromagnetic or antiferromagnetic contributions.

Figure 2(a) shows Raman spectra of $Ga_{1-x}Cr_xN$ measured by using the laser at 488 nm for excitation. The tested samples, #A to F, contained Cr in the range of $x = 0$–9% as denoted in the figure. According to XRD, not shown here, there was no phase separation for all the samples. For comparison, figure 2(a) contains spectra of high quality GaN (bottom) and ion-implanted GaN (top) as in figure 1(a). The E_2(high) and A_1(LO) phonon signals are sharply peaked at low Cr concentrations in $x = 0$–3% (#F, E, D), but slightly broadened at 3–5% (#C, B) and finally severely broadened at $x = 9.2\%$ (#A). The last sample (#A) shows a similar spectrum to that of an ion-implanted sample (top), thus its long-range lattice ordering is seriously deteriorated. It is clear anyway from the comparison between figures 1(a) and 2(a) that Cr has higher miscibility than Mn to GaN, and the wurtzite host-lattice structure is retained in the whole tested range of 0–9%.

EXAFS revealed that these spectral characteristics were strongly correlated with the local atomic arrangement around the impurity: Cr atoms substituted the Ga site and were tetrahedrally surrounded by N atoms at low Cr contents of $x < 3\%$ (#F, E, D), but at higher contents (#C, B, A) Cr atoms in the interstitial site increased and the local atomic arrangement shifted to the CrN-like structure (NaCl-type). Thus, broadening of the phonon peak is clearly correlated with the onset of Cr incorporation in the interstitial sites. The severely broadened spectrum of #A may be correlated with precipitation of secondary phases like CrN, though precipitation of the secondary phase was not clearly observed by Raman scattering and XRD.

At low Cr concentration (#C, D, E), a weak impurity mode appeared at 510 cm^{-1} as marked by the arrow in figure 2(a). This mode grew in intensity with the increase in Cr content and showed the same polarization property as peak (d) in GaMnN (see figure 1(a)), thus it may be assigned to LVM related to Cr in the Ga site, or, since the frequency is not simply explained by considering only the reduced-mass difference as the peak (d) for GaMnN, it may be attributed to defects of the host lattice induced by Cr incorporation. Furthermore, a low-doped sample #E shows an additional signal at about 535 cm^{-1}. This signal showed the same polarization property as the mode at 510 cm^{-1}, but its origin is not known. In a separate experiment on $Ga_{1-x}Eu_xN$ with $x = 2\%$, similar LVM was observed at 535 cm^{-1}. This suggests that this mode can appear irrespective of the impurity species, thus the modes around 510–535 cm^{-1} may be due to some host lattice defect. Another possibility is that the

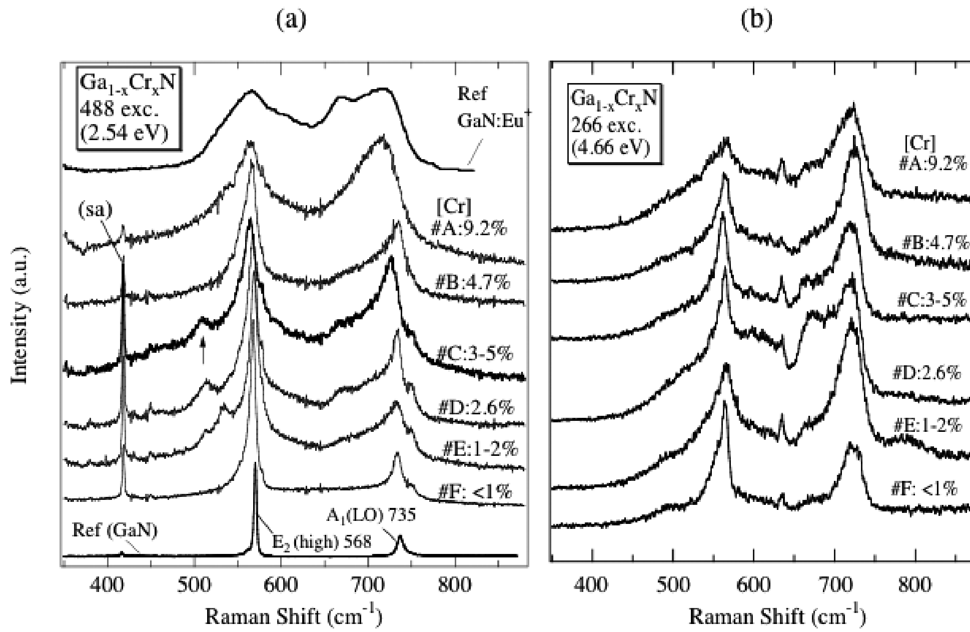

Figure 2. Raman spectra of $Ga_{1-x}Cr_xN$ observed with a visible laser (a), and a deep UV laser (b). For reference, (a) contains spectra of high quality GaN (#F) and ion-implanted GaN (#D) [10]. The arrow in (a) denotes an impurity mode. The sharp peak commonly observed in (b) at 640 cm^{-1} has instrumental origin.

535 cm^{-1} mode is assigned to the A_1(TO) phonon mode of GaN at 533 cm^{-1} [10]. This mode might be observed as a result of the disorder effect, though it should be forbidden in the present scattering geometry for ideal crystals.

Figure 2(b) shows Raman spectra of $Ga_{1-x}Cr_xN$ observed using a deep UV laser at 266 nm (4.66 eV) for excitation. Since the laser penetration depth to the sample is roughly 20–30 nm, only the topmost GaCrN layer is observed. It is easily noticed that the LO phonon signal is enhanced compared with the case of visible excitation. This is due to a resonant Raman effect induced by photo-excitation of free carriers, which indicates that the samples #B to F have well-defined band structure. (The sharp peak commonly observed at 640 cm^{-1} is a spurious signal due to instrumental origin, so it should be neglected.) We consider that photo-generation of free carriers in DMS has an important meaning for future applications to devices for optical control of ferromagnetism.

Once a resonant Raman effect occurs, Raman selection rule is relaxed and all longitudinal optic modes may be enhanced. The broadened LO-phonon spectra in #D, E and F may be attributed to simultaneous excitation of A_1(LO) and E_1(LO) modes. The sample #A shows, however, no such effect, probably because its band structure is obscured by heavy lattice damage.

3.2. ZnO doped with Ga + N (codoping), V and Co

Figure 3(a) shows Raman spectra of ZnO codoped with Ga and N. Here, the Ga content was varied from 0% (#G) to 8% (#A) as denoted in the figure (1 mol% = 4×10^{20} cm^{-3}). The undoped sample #G shows ZnO phonon signals at 332, 380, 437 and 570–580 cm^{-1}, corresponding to a second-order phonon, and first-order phonons of A_1(TO), E_2(high) and A_1,

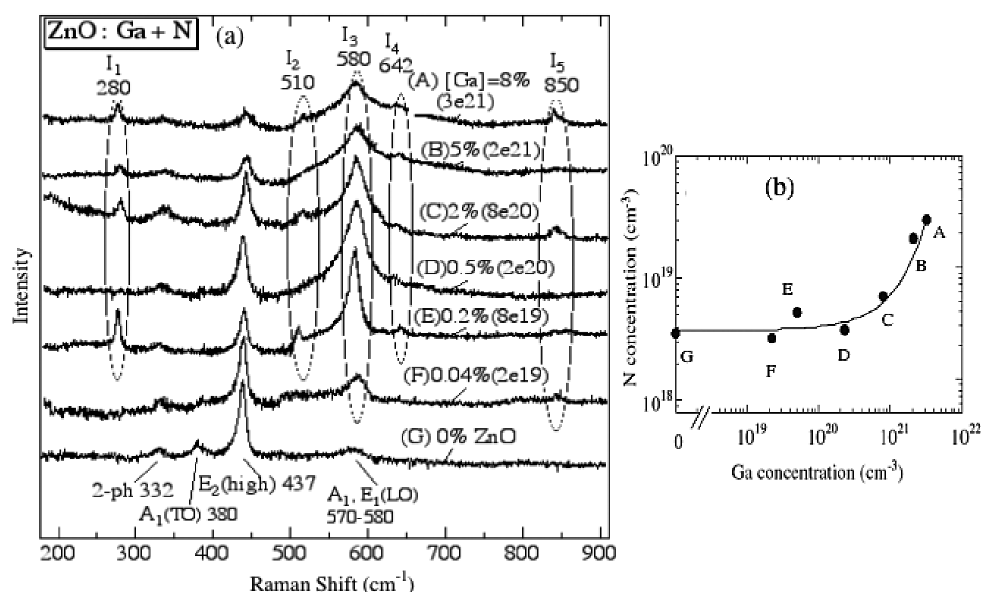

Figure 3. Raman spectra of ZnO codoped with Ga and N (a), and variation of N concentration along with Ga concentration (b). I_1–I_5 are impurity signals observed by doping. The marks A–G in (b) correspond to the samples #A–G in (a).

and/or E_1(LO), respectively. These spectral features indicate that the samples are polycrystal. It is easily observed that the E_2(high) and A_1(TO)-phonon modes weaken or disappear with the increase of Ga content, while five impurity modes I_1 to I_5 newly appear at 280, 510, 580, 642 and 850 cm^{-1}, respectively. These impurity modes are classified roughly to three groups by the dependence on the Ga content: first, the strongest signal, I_3, grows in peak height with the increase of Ga from 0 to 0.2% (#G to E), then slightly broadens at 0.5–2% (#D to C) and finally severely broadens at 5–8% (#B to A). The second group consists of I_1, I_2 and I_4, which are always sharp with constant relative intensity and appear in relatively lightly doped samples like #E. The third group includes I_5, which appear in relatively heavily doped samples like #A and #C.

Figure 3(b) shows the concentration of N incorporated to the ZnO layers along with Ga [9]. The N concentration begins to rise at [Ga] $\sim 2 \times 10^{20}$ cm^{-3} (=0.5%) from #D to #C, then rapidly increases at [Ga] $> \sim 8 \times 10^{20}$ cm^{-3} (=2%) from #C to #A. Clearly, this variation is strongly correlated with the broadening of the main impurity peak I_3 as described above. We consider therefore that the broadening of I_3 suggests the formation of complex centres, including N or related defects. Kaschner *et al* [14] first observed I_1 to I_5 in ZnO layers doped *only* with N ($<1.3 \times 10^{19}$ cm^{-3}). The signal intensities grew linearly with the N content, thus these authors assigned the signals to LVM of N. Later, however, Bundesmann *et al* [15] observed these modes in ZnO layers doped *not* with N but with *other* elements (Fe, Sb and Al). They therefore attributed these modes to host lattice defects. In our case, the latter view is supported because the signal intensities are not correlated with the N concentration. (The broadening of I_3 is correlated with the N content, however, as described above.) To summarize, all the tested ZnO samples maintain the wurtzite host-lattice structure since characteristic phonon signals are observed. However, many impurity modes appear with doping, which are due to host-lattice defects. Precise analysis of these modes remains a future subject.

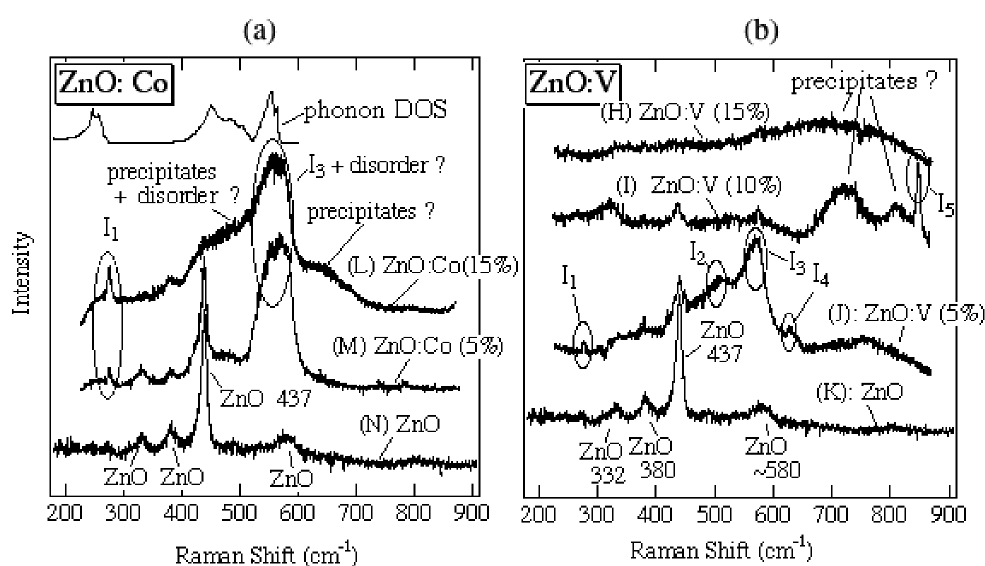

Figure 4. Raman spectra of ZnO doped with Co (a) and V (b). Impurity signals I_1–I_5 observed in figure 3 appears again in both figures. A calculated phonon DOS of ZnO [16] is re-plotted at the top of figure 4(a).

Figures 4(a) and (b) show Raman spectra of ZnO layers doped with Co and V, respectively. It is found that the impurity modes I_1 to I_5 observed in figure 3(a) appear again in the doped samples. Since these samples do not include nitrogen, the impurity modes should be attributed to the host lattice defects. For 5% doping of Co (sample #M) and V (sample #J), the host lattice phonon structure is well retained for both cases. However, since the host-lattice phonon spectrum is better reproduced in #M, cobalt seems more miscible than vanadium to ZnO. The broad signal in #J extending from about 400 to 600 cm^{-1} is a characteristic signal showing short-range lattice ordering as observed in #A and #B in figure 3(a). This is supported by the phonon-DOS calculations carried out by Serrano *et al* [16] as re-plotted at the top of figure 4(a). A similar DOS calculation was also reported by Kaschner *et al* [14]. Phase separation is clearly recognized when 10% of V is doped (#I). At 15% of impurity concentration, precipitate signals dominate the spectra for both V and Co, indicating that severe phase separation occur (#L, #H).

A separate experiment on magnetization in V-doped ZnO revealed that n-type samples were ferromagnetic at above room temperature [8].

4. Conclusion

Structural properties of GaN and ZnO layers doped with magnetic impurities were investigated by Raman scattering. Long-range lattice ordering and local atomic arrangement around magnetic impurities were analysed, and their solubility limit was considered. For GaN, magnetic elements of Mn and Cr are miscible roughly up to 1–2% and 3–5%, respectively. Here, they occupy the Ga site and form uniform solid solutions. In the case of ZnO, impurities of Co and V dissolve at least by ~5%. ZnO presents rich impurity signals deriving probably from host lattice defects, and the signals will be conveniently used for monitoring the doping process.

Acknowledgments

This work was performed by close collaboration with Professor Asahi, Professor Tabata and many other researchers at Osaka University and co-workers at Kyoto Institute of Technology. I deeply appreciate their kindness for supplying the samples, and for presenting many experimental data on the samples. Stimulating discussions with all these people as well as Professor Katayama-Yoshida are also acknowledged. This work was supported by the Ministry of Education, Culture, Sports, Science and Technology of Japan (MEXT), through MEXT Special Coordination Funds for Promoting Science and Technology (Nanospintronics Design and Realization, NDR).

References

[1] Dietl T, Ohno H, Matsukura F, Cibèrt J and Ferrand D 2000 *Science* **287** 1019
[2] Sato K and Katayama-Yoshida H 2000 *Japan. J. Appl. Phys.* **39** L555
[3] Pearton S J, Abernathy C R, Overberg M E, Thaler G T, Norton D P, Theodoropoulou N, Hebard A F, Park Y D, Ren F, Kim J and Boatner L A 2003 *J. Appl. Phys.* **93** 1
[4] McCluskey M D 2000 *J. Appl. Phys.* **87** 3593
[5] Yamamoto T and Katayama-Yoshida H 1999 *Japan. J. Appl. Phys.* **38** L166
[6] Hashimoto M, Zhou Y K, Tampo H, Kanamura M and Asahi H 2003 *J. Cryst. Growth* **252** 499
[7] Hashimoto M, Zhou Y K, Kanamura M, Katayama-Yoshida H and Asahi H 2003 *J. Cryst. Growth* **251** 327
[8] Saeki H, Tabata H and Kawai T 2001 *Solid State Commun.* **120** 439
[9] Matsui H, Saeki H, Tabata H and Kawai T 2003 *Japan. J. Appl. Phys.* **42** 5494
[10] Davydov V Yu, Kitaev Yu E, Goncharuk I N, Smirnov A N, Graul J, Semchinova O, Uffmann D and Evarestov R A 1998 *Phys. Rev.* B **58** 12899
[11] Limmer W, Ritter W, Sauer R, Mensching B, Liu C and Rauschenbach B 1998 *Appl. Phys. Lett.* **72** 2589
[12] Gebicki W, Strzeszewski J, Kamler G, Szyszko T and Podsiado S 2000 *Appl. Phys. Lett.* **76** 3870
[13] Zajac M, Doradziski R, Gosk J, Szczytko J, Lefeld-Sosnowska M, Kamiska M, Twardowski A, Palczewska M, Grzanka E and Gebicki M 2001 *Appl. Phys. Lett.* **78** 1276
[14] Kaschner A, Haboeck U, Strassburg M, Strassburg M, Kaczmarczyk G, Hoffmann A, Thomsen C, Zeuner A, Alves H R, Hofmann D M and Meyer B K 2002 *Appl. Phys. Lett.* **80** 1909
[15] Bundesmann C, Ashkenov N, Schubert M, Spemann D, Butz T, Kaidashev E M, Lorenz M and Grundmann M 2003 *Appl. Phys. Lett.* **83** 1974
[16] Serrano J, Manjón F J, Romera A H, Widule F, Lauck R and Cardona M 2003 *Phys. Rev. Lett.* **90** 55510